Pergamon

Chaos, Solitons & Fractals Vol. 9, No. 12, pp. 1931–1944, 1998

PII: S0960-0779(98)00008-3

Synchronization of Coupled Kicked Limit Cycle Systems

RICARDO L. VIANA[a,b]* and ANTÔNIO M. BATISTA[c]

[a] Institute for Physical Science and Technology, University of Maryland, College Park, MD, 20742, U.S.A.
[b] Departamento de Física, Universidade Federal do Paraná, 81531-990, Curitiba, PR, Brazil
[c] Departamento de Física, Universidade Estadual de Ponta Grossa, Ponta Grossa, PR, Brazil

(Accepted 6 January 1998)

Abstract—A class of kicked nonlinear limit cycle oscillators is described by a prototype circle map. We consider a spatially extended system in which these maps are coupled in a unidimensional lattice, according to a coupling scheme that includes the global (mean-field) and local (nearest-neighbor) prescriptions as limiting cases. We analyze frequency synchronization in the system, investigating its behavior under variations of the coupling parameters. © 1998 Elsevier Science Ltd. All rights reserved.

1. INTRODUCTION

Limit cycle systems appear in various problems in nonlinear dynamics, particularly in the analysis of relaxation oscillators, as the Van der Pol equation [1]. Limit cycle oscillators are also useful as phenomenological models for studies of the low-dimensional dynamics of the heart [2]. In chemical kinetics, the driven Brusselator and related models [3]; and in electronics, certain negative-resistance oscillators [4] are also limit cycle systems.

A question that has been addressed in many of these investigations refers to the behavior of limit cycle systems under an external, periodic perturbation. If the phase space of the unperturbed system is two-dimensional, a time-dependent perturbation can lead to different responses, like periodic, quasi-periodic, and chaotic motion. There are some techniques to explore the dynamical features of such systems, specially when the perturbation is a sequence of delta-function pulses.

It has been proposed that a isochrone portrait of limit cycle systems could provide a one-dimensional approximation for their Poincaré (stroboscopic) maps [5]. This map can be also drawn from a direct integration of the dynamical equations, taking into account the solution jump due to the delta-function pulses [6]. The reduction of the forced limit cycle oscillator to a low-dimensional map enables us to have some insights on the intricacies of the oscillator behavior, as well as to reduce the computer time by a significant amount, when compared with the numerical integration of the related differential equations.

* Author for correspondence.

Although the time evolution of such oscillators has been studied in depth over the past years, the question of how coupled oscillators behave in extended systems seems to be far from being completely answered, up to now. The use of coupled map lattices has been providing a useful new tool to investigate spatio-temporal dynamics, since it is possible to use the understanding of the low-dimensional temporal behavior of isolated system to extract information about the spatial structures created [7].

Coupled map lattices are dynamical systems with discrete space and time, and a continuous state variable. They have been intensively used as models for spatio-temporal phenomena, since it is possible to design systems with an arbitrarily large number of degrees of freedom, yet maintaining the inherent computational simplicity of maps. Map iterations give the time evolution of the system units, while lattice coupling provides diffusion and formation of complex spatial structures.

The phenomenology of CML is very rich, and includes solitons, kink and anti-kink propagation, periodic and frozen random patterns, space–time intermittency and fully developed turbulence [7, 8]. One of the most significant dynamical features is the possibility of synchronization: starting with an arbitrary spatial pattern, lattice coupling makes a given number of maps to synchronize in frequency or in phase. This may occur either for a limited number of sites or the entire lattice.

Synchronization of time–periodic systems has many applications in biological and physical systems. Certain species of fireflies, for example, flash collectively with a same period due to a synchronization process that make them adjust their own rhythms [9]. Arrays of coupled Josephson junctions have been used as reliable voltage standards, parametric amplifiers and millimeter wave generators. These quantum junctions have a distribution of their natural frequencies due to fluctuations in their microscopic parameters, like resistances and threshold currents. When coupled, the junctions may overcome their disordered frequencies and synchronize, yielding a power output that increases with the number of elements [10]. Other examples would include the collective behavior of specialized pacemaker cells in the human heart due to mutual synchronization, and circadian rhythms in general [11].

In this work, we study a prototype limit cycle oscillator with impulsive periodic forcing proposed by Ding [12, 13] as a one-dimensional circle map. We have added to each oscillator a natural frequency, in order to build assemblies of non-equal systems, which would represent a more realistic description of synchronization processes in nature. We consider a one-dimensional lattice of such maps with a variable range coupling similar to that introduced by Rogers and Wille [14] in a previous study of coupled continuous-time linear oscillators with nonlinear interaction. This coupling includes as particular cases previously studied prescriptions like the global 'mean-field' and local nearest-neighbor (diffusive) couplings.

Synchronized and non-synchronized states are distinguished by means of the winding number distribution for coupled sites and the order parameter of the lattice with periodic boundary conditions. Although it is possible to study phase synchronization in such lattices, we will restrict our discussion to frequency synchronization. In particular, we will not address the problem of phase synchronization of chaotic systems [15], since we use the winding number as a measure of the frequency of the coupled maps, and this concept is ill-defined within the realm of chaotic motion. In order to characterize synchronization we have used as diagnostics the mean square deviation of winding numbers, the order parameter time series, and a measure of the relative number of synchronization plateaus. We suggest the existence of a phase-transitional effect when the range parameter of the coupling is varied.

This paper is organized as follows: in the first section we present the prototype kicked limit cycle system to be studied, and the corresponding stroboscopic (Poincaré) map. The following section is devoted to a description of the coupled map lattice and some of its properties. In the third section we make a systematic study of frequency synchronization in the lattice with respect to variations in the coupling parameters. Our conclusions are left to the final section.

2. PROTOTYPE KICKED OSCILLATOR

The planar limit cycle system to be considered in this paper is given by (in polar coordinates $x = r\cos\theta$, $y = r\sin\theta$)

$$\frac{dr}{dt} = sr(1-r^2), \tag{1}$$

$$\frac{d\theta}{dt} = \Omega, \tag{2}$$

where $-\pi < \theta \leqslant \pi$ and $s > 0$ is a damping coefficient. $0 < \Omega \leqslant 1$ is a natural frequency for the oscillator (previous works [12, 16] have considered the case $\Omega = 1$). This system presents a stable limit cycle with unitary radius and an unstable fixed point at $r = 0$ (which characterizes a soft oscillator).

Perturbing this system by a sequence of delta-function kicks in the x-direction, with amplitude $2a > 0$ and frequency $b \in (0,1]$ we rewrite eqn (1) and eqn (2) as

$$\frac{dx}{dt} = sx(1-x^2-y^2) - y\Omega + 2a\sum_{n=-\infty}^{\infty}\delta(t-2\pi nb), \tag{3}$$

$$\frac{dy}{dt} = sy(1-x^2-y^2) + x\Omega. \tag{4}$$

A stroboscopic (time–$2\pi b$) map can be obtained from the above equations as follows: let r_n and θ_n denote the radial and angular variables just after the n-th kick.

$$r_n = \lim_{\varepsilon\to 0} r(t = 2\pi nb + \epsilon),\ \theta_n = \lim_{\varepsilon\to 0}\theta\,(t = 2\pi nb + \epsilon). \tag{5}$$

Integration of eqn (3) and eqn (4) is performed in two steps: between two successive kicks (where there is no perturbation, so the solution is quite simple); and over the neighborhood of a delta function (where we evaluate the jump of both variables). Details of the calculation can be found in Ref. [12]. Proceeding in this way, one obtains the two-dimensional dissipative map

$$r_{n+1} = [(r_n^* \cos(\theta_n + 2\pi b\Omega) + 2a)^2 + (r_n^* \sin(\theta_n + 2\pi b\Omega))^2]^{1/2}, \tag{6}$$

$$\tan\theta_{n+1} = \frac{r_n^* \sin(\theta_n + 2\pi b\Omega)}{2a + r_n^* \cos(\theta_n + 2\pi b\Omega)}, \tag{7}$$

where

$$r_n^* \equiv \frac{r_n}{[r_n^2 + (1-r_n^2)\exp(-4\pi sb)]^{1/2}} \tag{8}$$

denotes the value of r immediately before the $(n+1)$-th kick.

Note that s is a measure of the inverse relaxation time when perturbations drive the phase point out of the unperturbed limit cycle. For fast relaxation ($s \to \infty$), each kick displaces the phase point from the unperturbed limit cycle, but it returns immediately, i.e., radially (and always before the next kick). In this limiting case $r_n^* \to 1$, so that eqn (7) is reduced to a circle map $\theta \mapsto f(\theta)$, with f: $(-\pi,\pi] \to (-\pi,\pi]$, and

$$\tan\theta_{n+1}=\frac{\sin(\theta_n+2\pi b\Omega)}{2a+\cos(\theta_n+2\pi b\Omega)}. \tag{9}$$

This circle map is prototypical in the sense that it is a simple dynamical system containing typical parameters of periodically forced limit cycle systems: the amplitude $2a$ and combined frequency $\beta\equiv b\Omega$. It has been studied by Ding [13] and Ullmann and Caldas [16]. In the parameter space a–β there are two basic dynamical regimes. For $0\leqslant a<1/2$ ('weak force' region) the map (9) is invertible and we have the usual Arnold's tongue structure, with mode-locking and quasi-periodic regions, characterized by the winding number

$$w=\frac{1}{2\pi}\lim_{n\to\infty}\frac{f^n(\theta_0)-\theta_0}{n}. \tag{10}$$

In the invertible region the limit above always exists and does not depend on the initial condition θ_0 [17]. A mode-locking region is a set of points in the parameter space for which the winding number is a given rational $w=\tilde{p}/\tilde{q}$, where $\tilde{p}$ and $\tilde{q}$ are co-prime integers. Accordingly, quasi-periodic regions are characterized by irrational winding numbers.

For $1/2<a<1$ the map is non-invertible and there are two distinct sub-regions: a unimodal sub-region, where the map may present chaotic behavior for some parameter ranges, and an intermediate sub-region characterized by periodic orbits. Ullmann and Caldas [16] have studied the transitions between these regimes. For example, for $0.540\leqslant a\leqslant 0.610$ and $\beta=0.315$, the map presents an inverse period doubling cascade leading to chaotic behavior intermingled with periodic windows [18]. In the chaotic regime the limit appearing in eqn (10) does not exist in general, and the winding number no longer provides a good characterization for orbits.

3. COUPLED PROTOTYPE MAP LATTICES

Lattice coupled dynamical systems are models for studies of spatio-temporal complexity, including turbulent behavior. A special category of these systems includes coupled map lattices (CML), that are characterized by a discrete space (lattice), whose sites are occupied by maps with a continuous state variable undergoing discrete time evolution.

CML may present spatially extended structures, like domains, in which sites are in-phase, separated by kink and anti-kink pairs, which form domain walls. These walls may move along the lattice, according to the coupling strength, and interact with other kink-anti-kink pairs.

Coupled circle maps have been studied as models for describing mode locking in charge–density wave materials [19], and attractor crowding in arrays of coupled Josephson junctions with noise [10]. In the latter case, it has been found that they may also present chaotic itineracy—the switching between quasi-stationary high-dimensional chaotic motion and low-dimensional attractor remnants [20].

Coupled sine–circle maps, for which $\theta\mapsto\theta+\Omega+(K/2\pi)\sin(2\pi\theta)$, were first used [7] to show the existence of soliton turbulence in coupled map lattices. Soliton turbulence is characterized by aperiodic behavior caused and sustained by kink-anti-kink collisions and the creation and annihilation of these pairs. Incidentally, the prototype map (9) reduces to the sine–circle map for small amplitude a [12]. The spatio-temporal patterns seen in sine–circle map lattices are similar to those observed in damped sine–Gordon partial differential equation with periodic forcing.

Consider a one-dimensional lattice of N sites. We will denote $\theta_n^{(i)}$ the value of the state variable θ in the site i ($i=0,1,2,\ldots,N-1$) at time n ($n=0,1,2,\ldots$). Periodic boundary conditions are supposed: $\theta_n^{(i)}=\theta_n^{(i\pm N)}$. The initial conditions profile to be considered will be a random distribution

of iterates between $-\pi$ and $+\pi$. A particular specification of initial conditions, while could influence the lattice pattern at a given time, does not affect our results concerning winding number computations.

Each site can be coupled with its neighbors in several ways. The so-called local couplings involve only nearest-neighbor sites, like the Laplacian future prescription

$$\theta_{n+1}^{(i)} = f(\theta_n^{(i)}) + \frac{\epsilon}{2}[f(\theta_n^{(i+1)}) - 2f(\theta_n^{(i)}) + f(\theta_n^{(i-1)})], \tag{11}$$

where $f(\theta)$ is the prototype map (9), and ϵ is the coupling strength. The coupling term may be viewed as the discretization of a second derivative, hence the term Laplacian for it. As the coupling is applied after the action of the map function, it is also called future.

However, if we are to describe a lattice of nonlinear limit–cycle oscillators subjected to a same kind of external perturbation, represented by the amplitude and frequency of the impulsive forcing, it would be more convenient to couple the oscillator phases *before* applying the map. Our local coupling would assume the form

$$\theta_{n+1}^{(i)} = f\left[\theta_n^{(i)} + \frac{\epsilon}{2}(\theta_n^{(i+1)} - 2\theta_n^{(i)} + \theta_n^{(i-1)})\right], \tag{12}$$

and has essentially the same dynamics of the previous form [8].

Global couplings involve all lattice sites in the same foot, regardless of their relative positions, taking into account their average contribution on a given site. It is also referred as a 'mean-field' prescription. According our convention of updating the lattice before the map iteration, we write this coupling as

$$\theta_{n+1}^{(i)} = f\left[(1-\epsilon)\theta_n^{(i)} + \frac{\epsilon}{N-1}\sum_{\substack{j=1 \\ j\neq i}}^{N}\theta_n^{(i)}\right], \tag{13}$$

In order to study the transition between local and global couplings, we shall use a variable range coupling [14], in which the interaction between sites decreases with the lattice distance in a power-law fashion:

$$\theta_{n+1}^{(i)} = f\left[\theta_n^{(i)} + \frac{\epsilon}{\eta(\alpha)}\sum_{j=1}^{N'}\frac{1}{j^{\alpha}}(\theta_n^{(i+j)} - 2\theta_n^{(i)} + \theta_n^{(i-j)})\right], \tag{14}$$

where $N' = (N-1)/2$, and

$$\eta(\alpha) = 2\sum_{j=1}^{N'}\frac{1}{j^{\alpha}} \tag{15}$$

is a normalization factor. It comes from the fact that the summation in eqn (14) is actually a weighted average of terms $\theta_n^{(i+j)} - 2\theta_n^{(i)} + \theta_n^{(i-j)}$, the factor $\eta(\alpha)$ being the sum of the corresponding statistical weights.

Let us consider the limiting cases of the above prescription. For $\alpha = 0$ we have $\eta = N-1$ and we may rewrite the summation in such a way that we obtain the global mean-field coupling (13). If $\alpha \to \infty$ only the terms with $j=1$ survive in both summations. Hence $\eta \to 2$ and only the nearest-neighbor sites contribute to the coupling, resulting in the local Laplacian coupling (12).

Now let α be a positive real number. We may rewrite the coupling as $\theta_{n+1}^{(i)} = f[\theta_n^{(i)} + \epsilon \mathscr{I}^{(i)}(\alpha, \theta_n)]$, where we introduce an interaction term

$$\mathscr{I}^{(i)}(\alpha,\theta_n)=\frac{1}{\eta(\alpha)}\sum_{j=1}^{N'}\frac{1}{j^{\alpha}}(\theta_n^{(i+j)}-2\theta_n^{(i)}+\theta_n^{(i-1)}), \tag{16}$$

where $\theta_n=(\theta_n^{(0)},\theta_n^{(1)},\ldots\theta_n^{(N-1)})$ is the lattice pattern at time n. It is identically null for sites inside a domain where all maps are in-phase, i.e. have the same value for the state variable at a given instant of time.

A linear distribution for the state variable $\theta_n^{(i)}=\xi i$ (where ξ is a constant, for example equal to π/N) would also give a vanishing interaction term for all sites, since $\theta_n^{(i-j)}-2\theta_n^{(i)}+\theta_n^{(i+j)}=\xi(i-j-2i+i+j)=0$. It is very difficult to give analytical expressions for $\mathscr{I}^{(i)}$, except in some particular cases, like the quadratic distribution $\theta_n^{(i)}=(2/N)^2 i^2$. The interaction term, that depends only on α (i.e., it is the same for all sites), reads

$$\mathscr{I}^{(i)}(\alpha)=\frac{4}{N^2}\frac{\sum_{j=1}^{N'}j^{2-\alpha}}{\sum_{j=1}^{N'}j^{-\alpha}},$$

so that its magnitude decreases exponentially with α. Although in a subsequent instant the lattice distribution is no longer of this form, due to lattice updating, we may expect that large values of α should always give a relatively small contribution in terms of coupling. This has also been verified for a random distribution of iterates (with zero mean), for which $\mathscr{I}^{(i)}(\alpha)$ is well fitted by a Gaussian function, and vanishes when an average over the lattice is taken.

4. SYNCHRONIZATION IN COUPLED PROTOTYPE LATTICES

Synchronization was discovered in 1665 by Huyghens for oscillations of two coupled pendula. In spite of its long history, it is still a subject of intense investigation in view of modern developments in the theory of coupled oscillating limit cycle systems and its various practical applications [11]. Here we have to distinguish between two distinct kinds of phenomena:

(i) Frequency synchronization: classically defined as the adjustment of the frequencies of periodic oscillators due to weak interaction [21];
(ii) Phase synchronization: occurs due to a strong interaction of an assembly of identical chaotic systems, whose states coincide at all times [15]. This type of synchronization among globally coupled logistic maps was shown to be related to the stable periodic windows of the isolated maps [22].

Although it is possible in principle to observe the latter type in coupled prototype lattices, we will focus on the first approach. We consider two or more maps (sites) to be frequency-synchronized if their winding numbers are equal (up to a specified tolerance). For coupled maps we should use the following expression for the winding number of the i-th site

$$w^{(i)}=\frac{1}{2\pi}\lim_{m\to\infty}\frac{1}{m-m_0}\sum_{n=m_0}^{m-1}\theta_{n+1}^{(i)}-\theta_n^{(i)}, \tag{17}$$

where m_0 is the number of transient iterations.

The set of $w^{(i)}$, for $i=0,1,2,\ldots, N-1$, defines a winding number profile. In absence of coupling this 'perturbed' winding number coincides with that given by eqn (10), and for vanishing kick amplitude ($a=0$) it also coincides with the natural frequencies $\Omega^{(i)}$ of the individual oscillators.

If each system unit were identical, i.e., with the same value of $\Omega^{(i)}$, the synchronization process would be very simple. However, consider the case in which each individual unit has a different value of $\Omega^{(i)}$ chosen at random between 0 and 1. Then the combined frequency $\beta^{(i)} = b\Omega^{(i)}$ will be also randomly distributed between 0 and b. This approach has been used in the study of phase synchronization in a lattice of non-identical Rössler oscillators [23].

Now the problem becomes more involved, since there are two basic processes in competition: (i) the inherent natural frequency, that is fixed in time for each oscillator, tends to lock the winding number in some value, that may be rational or irrational (for $a > 0$, the presence of Arnold tongues implies that there is a nonzero probability of obtaining rational winding numbers); (ii) the diffusion caused by spatial coupling tends to smooth individual effects caused by natural frequencies and bring a cluster of oscillators to behave with the same period, making them synchronize.

The competition between these factors becomes apparent when $\Omega^{(i)}$ are randomly chosen, since if there is synchronization between a given number of sites it is because the coupling-induced diffusion has overcome the inherent 'frozen' disordered behavior. The outcome will depend on the coupling properties.

In order to investigate this dependence, we have used some quantities to characterize synchronization. Due to the uniform random distribution of the natural frequencies, for sufficiently strong coupling, all sites tends to synchronize at a common frequency that approaches the value $b/2$. Thus we have computed for a given winding number profile both the average winding number $\langle w \rangle = (1/N)\Sigma_i w^{(i)}$, and the dispersion around this value

$$\delta w = \left[\frac{1}{N-1} \sum_{i=0}^{N-1} (w^{(i)} - \langle w \rangle)^2 \right]^{1/2}. \tag{18}$$

Figure 1 shows a series of winding number profiles obtained for a $N = 100$ lattice with global mean-field coupling ($\alpha = 0$) and different values of the coupling strength ϵ. The map parameters are $a = 0.4$ and $b = 1.0$, and we use different uniform random distributions for the natural frequencies $\Omega^{(i)}$ and the initial conditions profile $\theta_0^{(i)}$. In this way $0 < \beta^{(i)} \leqslant 1$ and we always work in the weak-force region of the parameter space for each site, avoiding chaotic orbits. For strong coupling [Fig. 1(a)] we see complete synchronization of all lattice sites at the value $\langle \mathrm{w} \rangle = 0.5$ with a dispersion less than 10^{-6}. As the coupling strength decreases [Fig. 1(b)] we observe the breaking of complete synchronization in some places, which become more numerous for smaller ϵ [Fig. 1(c)], but still having many clusters of synchronized states, which is a characteristic feature of global coupling. For very weak coupling [Fig. 1(d)], the number of such clusters is small, but with the same mean tendency, with a dispersion less than 20%.

Another diagnostic of synchronization is the order parameter, introduced by Kuramoto [11]. Let $\theta_n^{(i)}$, ($i = 0,1,2,..., N-1$) be the lattice pattern at time n. The complex order parameter is defined for our CML as

$$z_n = R_n \, \mathrm{e}^{i\varphi_n} \equiv \frac{1}{N} \sum_{j=0}^{N-1} \exp(i\theta_n^{(j)}). \tag{19}$$

The order parameter was originally introduced for chains of oscillators described by continuous-time models, in which synchronized states are characterized by a fixed value of the magnitude R (for infinite lattices) or fluctuations around this value of amplitude proportional to $1/\sqrt{N}$ (for finite chains). For non-synchronized states these oscillations continue to occur, but: (a) its behavior has complex periodicity; (b) its mean value is slightly less than in a synchronized state.

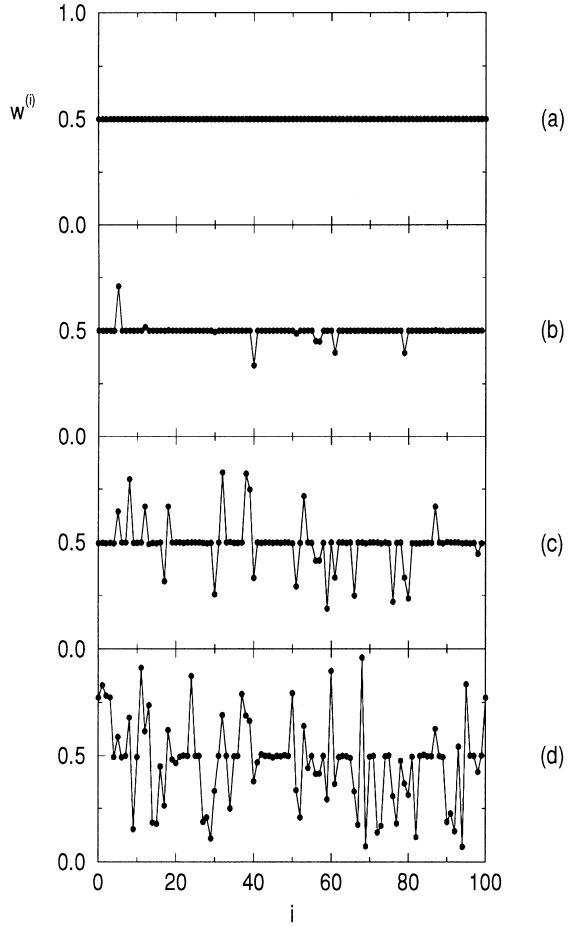

Fig. 1. Winding number profile for a $N=100$ lattice of prototype maps with $a=0.4$ and $b=1.0$. Natural frequencies $\Omega^{(i)}$ have a uniform random distribution. Coupling parameters are $\alpha=0$ and: (a) $\epsilon=0.90$, (b) $\epsilon=0.70$, (c) $\epsilon=0.50$, (d) $\epsilon=0.01$.

In order to characterize the temporal evolution of the order parameter magnitude we have used its power spectrum. Fig. 2 presents both the order parameter magnitude R_n and its corresponding power spectrum for the same parameter values of Fig. 1. While most of the lattice sites are synchronized [Fig. 2(a,b)], R_n undergoes regular oscillations, characterized by a small number of sharp frequency peaks in their power spectra. The breaking of this situation [Fig. 2(c,d)] is followed by an increasing complexity in the order parameter oscillations, whose mean value is slightly decreased, and with various additional frequency peaks in their spectra indicating the presence of many higher harmonics of the oscillation.

In practice, a modest value of the range parameter is already sufficient to give a local quasi-nearest-neighbor coupling. In Figs 3 and 4 we show winding number profiles and the respective order parameter magnitudes and spectra for $\alpha=3$. The differences with the global coupling are striking, since even for a strong coupling we have only a few synchronization plateaus [Fig. 3(a)]; giving irregular fluctuations in the order parameter magnitude with a noisy power spectrum without distinct frequency peaks [Fig. 4(a)].

For smaller coupling strengths [Fig. 3(b,c)] the situation is quite similar, with growth of the winding number dispersion, even though we still see some plateaus with small lengths (less than

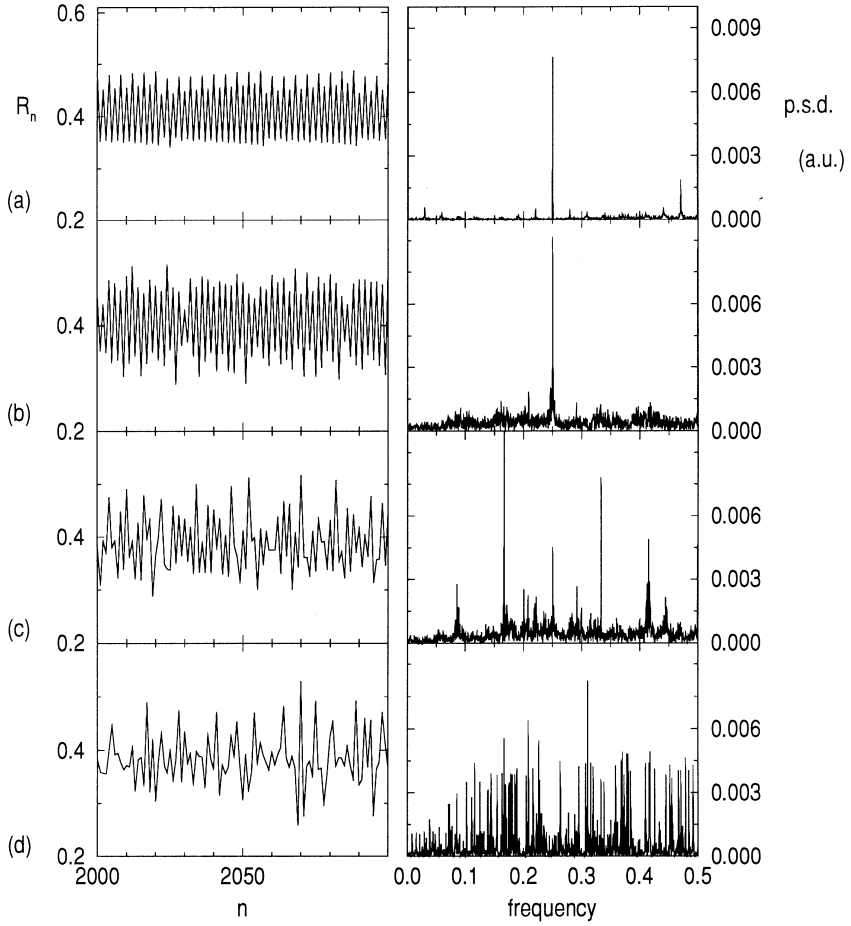

Fig. 2. Order parameter magnitude and corresponding power spectral density for the same parameters as the previous figure: $\alpha = 0$ and (a) $\epsilon = 0.90$, (b) $\epsilon = 0.70$, (c) $\epsilon = 0.50$, (d) $\epsilon = 0.01$.

5% of the lattice size), the same observation being valid for the corresponding power spectra [Fig. 4(b,c)]. For a very small coupling [Fig. 3(d)] the winding number distribution is similar to that for global coupling, as expected. Comparing Fig. 2(d) and Fig. 4(d), we see a very similar spectral content for order parameter fluctuations in both cases.

In local couplings the relative influence of lattice diffusion is small, and it is not enough to overcome the frozen disorder of the natural frequencies of each map. Thus, even if we use large coupling strengths, the overall result in terms of synchronization clustering is the roughly the same. The influence of range on the winding number profiles can be inferred from Fig. 5, where we have shown such profiles for different values of α and the same coupling strength. The transition from a completely synchronized state (Fig. 5(a), global coupling) to a completely non-synchronized state (Fig. 5(d), local coupling) is accomplished through breaking of the clustering structure. Initially the large plateau at 0.5 is broken [Fig. 5(b)], and besides the irregularities that remind us of the frozen natural disorder, there are also small plateaus at different winding number values [Fig. 5(c)].

In order to provide a characterization of this transition, we count the number of synchronization plateaus in these winding number profiles. Let N_i the length of the i-th plateau, and

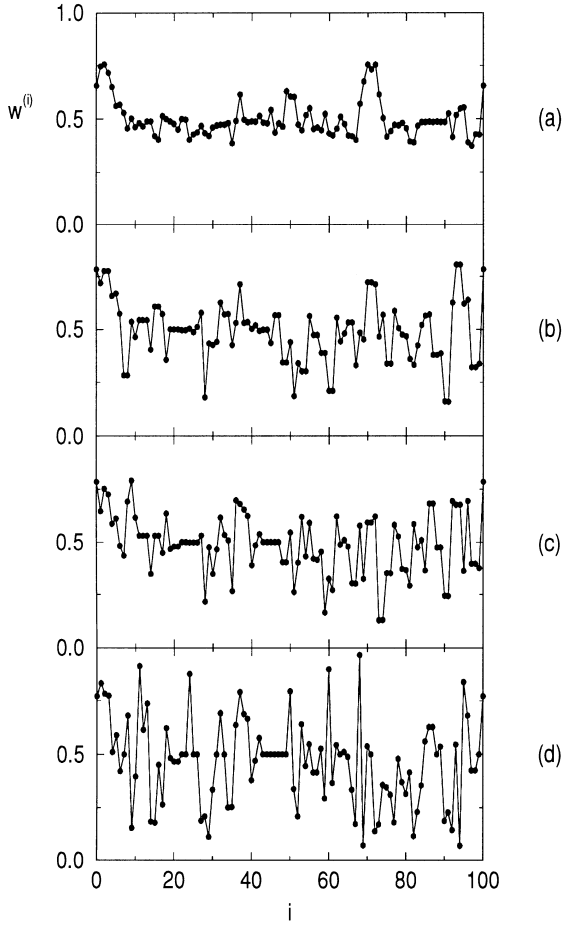

Fig. 3. Winding number profile for a $N=100$ lattice of prototype maps with $a=0.4$ and $b=1.0$. Natural frequencies $\Omega^{(i)}$ have a uniform random distribution. Coupling parameters are $\alpha=3$ and: (a) $\epsilon=0.90$, (b) $\epsilon=0.70$, (c) $\epsilon=0.50$, (d) $\epsilon=0.01$.

N_p the total number of plateaus. The mean plateau size being $\langle N\rangle$, the degree of synchronization is defined as

$$p=\frac{\langle N\rangle}{N}=\frac{1}{NN_p}\sum_{i=1}^{N_p}N_i. \tag{20}$$

For a completely synchronized state, as in Fig. 5(a), we have just one plateau (the entire lattice), so $\langle N\rangle=N$, and $p=1$. If we have a completely non-synchronized lattice there are almost as many plateaus as sites, so $N_p\approx N$, or $\langle N\rangle\approx 1$. Hence $p\approx 1/N\to 0$ for $N\to\infty$.

Figure 6(a) shows the variation of the winding number dispersion with the range parameter alpha, for the same parameters as Fig. 5 but considering more values of α. There is a rather abrupt transition between single-plateau states, in which δw is very small ($\approx 10^{-5}$), to non-synchronized states with a dispersion of the order of 10% of the winding number range. This conclusion is supported by Fig. 6(b), where we depict the degree of synchronization p corresponding to this case. The jump between a completely synchronized and non-synchronized states occurs for a coupling range value slightly less than 1.0. This phase transitional phenomenon has been found in chains of linear continuous-time oscillators with nonlinear interactions [14],

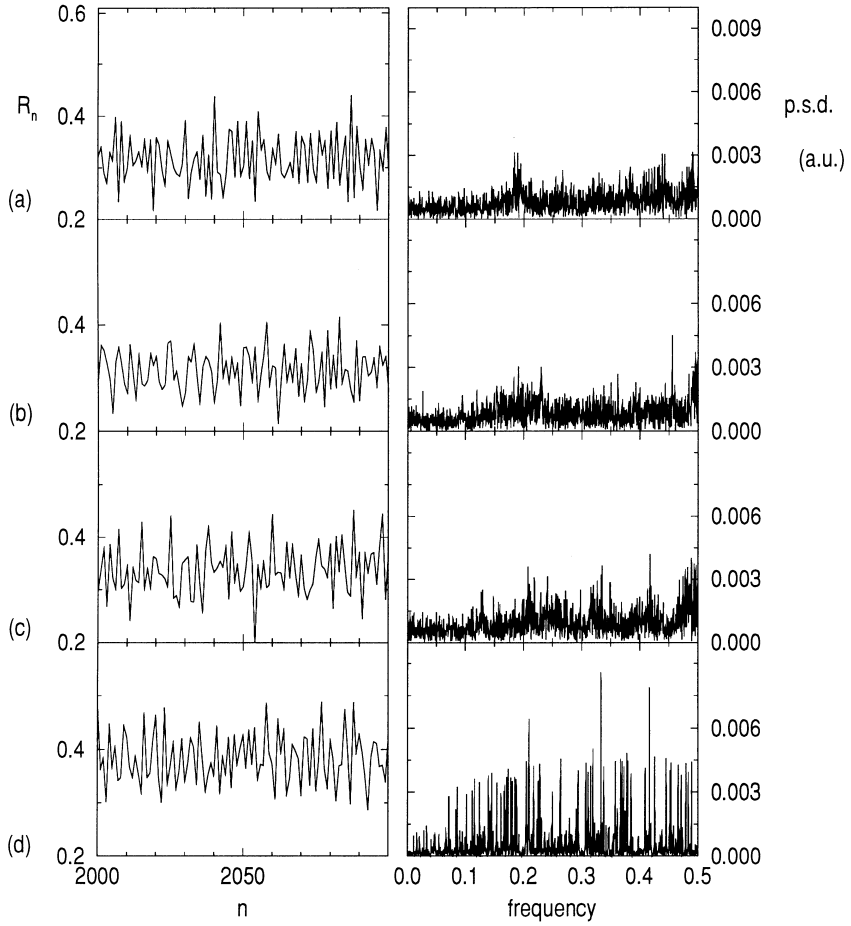

Fig. 4. Order parameter magnitude and corresponding power spectral density for the same parameters as the previous figure: $\alpha = 3$ and (a) $\epsilon = 0.90$, (b) $\epsilon = 0.70$, (c) $\epsilon = 0.50$, (d) $\epsilon = 0.01$.

where the corresponding critical value of α was found to be in accordance with a theoretical model due to Kuramoto [11].

5. CONCLUSIONS

Coupled nonlinear limit cycle oscillators have many applications in physical and biological sciences, and have received much attention in recent years. Although there are some exactly soluble models for such dynamical systems, one has frequently to rely on numerical simulations. For systems of coupled ordinary differential equation this task becomes computer intensive with increasing number of systems. So, the possibility of describing a certain class of these systems, namely kicked limit–cycle oscillators, by analytical low-dimensional mappings, is a convenient tool for visualizing the essential dynamics using less computer time.

In this work we have considered a prototype circle map for this study, and we have included a natural frequency for each oscillator, in such a way that we can couple unequal kicked oscillators subjected to the same impulsive perturbation. We have used a uniform random distribution of

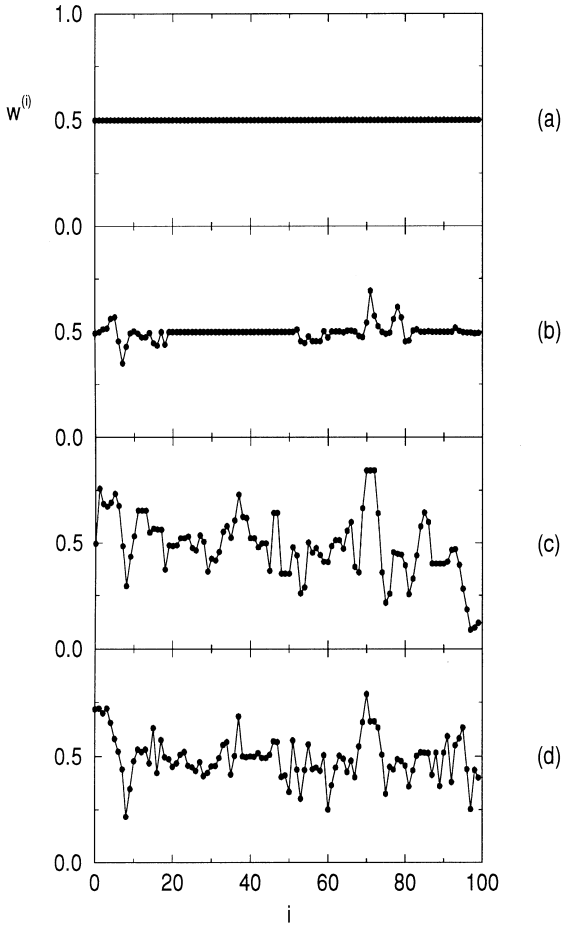

Fig. 5. Winding number profile for a $N=100$ lattice of prototype maps with $a=0.4$ and $b=1.0$. Natural frequencies $\Omega^{(i)}$ have a uniform random distribution. Coupling parameters are $\epsilon=0.85$ and: (a) $\alpha=0.0$, (b) $\alpha=1.0$, (c) $\alpha=2.0$, (d) $\alpha=3.0$.

natural frequencies for these maps. Parameters were chosen to yield periodic or quasi-periodic responses, ruling out chaotic behavior.

The resulting map lattice was endowed with a coupling depending on two parameters: the strength and the range. This range parameter enables us to go from the global 'mean-field' to the local 'nearest-neighbor' case. The coupling may be considered as a weighted average of the discretized second spatial derivative, the statistical weights being a decreasing power-law function of the lattice distance.

We have focused our attention on frequency synchronization, which shows up in the winding number profiles for the lattice. We have considered for characterization of synchronization: (a) the winding number dispersion; (b) the order parameter, and (c) the relative average plateau length.

For low values of the coupling range, the coupling is essentially of a global nature, in which all sites interact in a significant way with each map. A large diffusion effect is expected in such couplings, and indeed we have observed that synchronization is easier in this situation, unless a very small coupling strength is used. This is reflected in the small dispersions observed around the mean winding number.

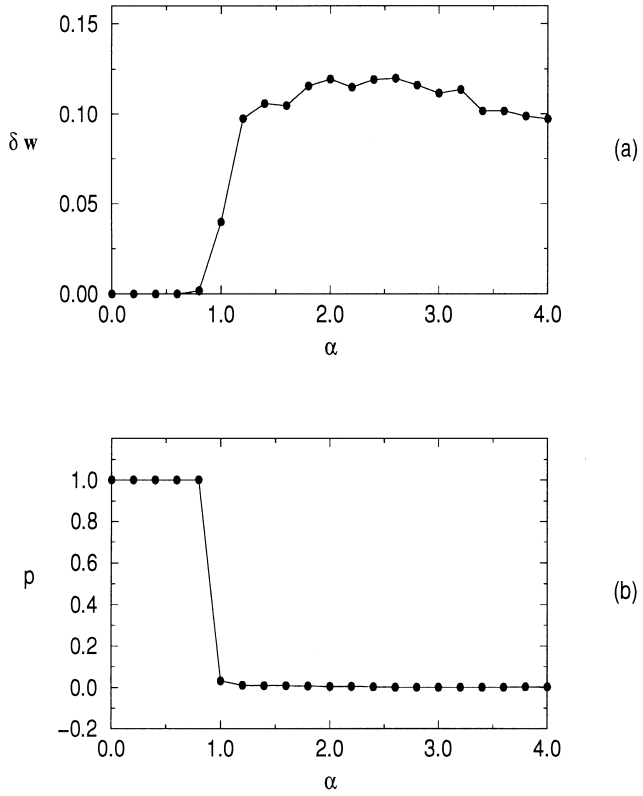

Fig. 6. Winding number dispersion (a), and relative average plateau length (b) of a winding number distribution for several values of the range parameter α and a fixed coupling strength $\epsilon = 0.85$. We consider a $N = 100$ lattice of prototype maps with $a = 0.4$, $b = 1.0$, and randomly distributed natural frequencies.

The order parameter for synchronized states is a complex number whose magnitude is a sum of contributions from the various sites, and with a fairly regular behavior in synchronized lattices. Power spectral analysis reveals the presence of a few frequency peaks characterizing periodic fluctuations. This is consistent with the finite size of the lattice, since we do not work in the thermodynamical limit.

Conversely, for bigger values of α the coupling is local and the diffusion effect is rather limited. In particular, it is not sufficiently strong to over-pass the frozen random disorder of the natural frequencies, so synchronization is considerably more difficult to occur, unless very strong coupling is used. Being typical for these cases, non-synchronized states have an irregular and highly complex, yet non-chaotic (as shown in power spectra) behavior for the order parameter magnitude.

The transition between these two limiting situations seems to be rather abrupt, as indicated by the sharp increase of winding number dispersion and the corresponding drop of the relative average plateau length in the vicinity of $\alpha = 1$. This kind of phase transition is similar to that observed in oscillator chains described by continuous-time (ordinary differential equations)models. We are currently investigating the nature of this phase transition, particularly with respect to the behavior near criticality, and its dependence on the other map and coupling parameters.

Acknowledgements—R. L. V. would like to acknowledge Prof. Celso Grebogi and Prof. James A. Yorke for the kind hospitality at IPST, University of Maryland, where most of this work was completed; and Drs. E. Macau and M. S.

Baptista for useful discussions. R. L. V. was partially supported by CNPq (Conselho Nacional de Desenvolvimento Científico e Tecnológico), Brazil and National Science Foundation, United States, through a joint research project. A.M.B. was supported by CAPES, Brazil.

REFERENCES

1. Steeb, W.-H., Kunick, A., Chaos in limit–cycle systems with external periodic excitation. *International Journal of Nonlinear Mechanics*, 1987, **22,** 349.
2. Glass, L. and Shrier, A., Low-dimensional dynamics in the heart. In *Theory of Heart*, ed. L. Glass, P. Hunter and A. McCulloch. Springer Verlag, N.Y., 1991.
3. Kai, T., Tomita, K., Stroboscopic phase portrait of a forced nonlinear oscillator. *Progress of Theoretical Physics*, 1979, **61,** 54.
4. Ueda, Y., Akamatsu, N., Chaotically transitional phenomena in the forced negative-resistance oscillator. *IEEE Transactions on Circuits and Systems*, 1981, **28,** 217.
5. Campbell, A., Gonzalez, A., Gonzalez, D. L., Piro, O., Larrondo, H. A., Isochrones and the dynamics of kicked oscillators. *Physica A*, 1989, **155,** 565.
6. Caldas, I. L., Tasso, H., Limit cycles of periodically forced oscillations. *Physics Letters A*, 1989, **135,** 264–266.
7. Crutchfield, J. P. and Kaneko, K., Phenomenology of spatio–temporal chaos. In *Directions in Chaos*, ed. B.-L. Hao, Vol. 1. World Scientific, Singapore 1987.
8. Kaneko, K., The coupled map lattice. In *Theory and applications of coupled map lattices*, ed. K. Kaneko. Wiley, Chichester, 1993.
9. Strogatz, S. H., Stewart, I., Coupled oscillators and biological synchronization. *Scientific American*, 1993, **269,** 102.
10. Wiesenfeld, K., Hadley, P., Attractor crowding in oscillator arrays. *Physical Review Letters*, 1989, **62,** 1335–1338.
11. Kuramoto, Y., *Chemical oscillations*, *waves*, *and turbulence*. Springer–Verlag, Berlin, 1984.
12. Ding, E. J., Analytical treatment of a driven oscillator with a limit cycle. *Physical Review A*, 1987, **35,** 2669–2683.
13. Ding, E. J., Structure of the parameter space for a prototype nonlinear oscillator. *Physical Review A*, 1987, **36,** 1488.
14. Rogers, J. L., Wille, L. T., Phase transitions in nonlinear oscillator chains. *Phys. Rev. E*, 1996, **54,** R2193–R2196.
15. Carroll, T. L., Heagy, J. F., Pecora, L. M., Transforming signals with chaotic synchronization. *Physical Review E*, 1996, **54,** 4676.
16. Ullmann, K., Caldas, I. L., Transitions in the parameter space of a periodically forced dissipative system. *Chaos*, *Solitons and Fractals*, 1996, **7,** 1913–1921.
17. Bak, P., Bohr, T. and Jensen, M. H., Circle maps, mode-locking and chaos. In *Directions in Chaos*, ed. B.-L. Hao, Vol. 2. World Scientific, Singapore, 1987.
18. Batista, A. M., M.Sc. Dissertation. Universidade Federal do Paraná, 1996, (unpublished).
19. Alstrøm, P., Ritala, R. K., Mode locking in an infinite set of coupled circle maps. *Physical Review A*, 1987, **35,** 300–312.
20. Kaneko, K., Globally coupled circle maps. *Physica D*, 1991, **54,** 5–19.
21. Pikowsky, A. S., Rosenblum, M. G., Osipov, G. V., Kurths, J., Phase synchronization of chaotic oscillators by external driving. *Physica D*, 1997, **104,** 219–238.
22. Shinbrot, T., Synchronization of coupled maps and stable windows. *Physical Review E*, 1994, **50,** 3230–3233.
23. Osipov, G. V., Pikowsky, A. S., Rosenblum, M. G., Kurths, J., Phase synchronization effects in a lattice of non identical Rössler oscillators. *Physical Review E*, 1997, **55,** 2353–2361.